8 Controlling Transient Chaos on Chaotic Saddles

T. Tél[1], Y.-C. Lai[2], and C. Grebogi[3]

1. Institute for Theoretical Physics, Eötvös University, H-1088 Budapes
u. 5-7, Hungary
2. Departments of Physics and Astronomy and of Mathematics, Uni
Kansas, Lawrence, Kansas 66045, USA.
3. Institute for Plasma Research, Department of Mathematics, Institute
ical Science and Technology, University of Maryland, College Park, M
USA

8.1 Introduction

Chaotic saddles are invariant *nonattracting chaotic sets* in the state spa
namical systems [1]-[6]. They are the fractal analog of saddle points chara
isolated unstable behaviors. In contrast to saddle points, chaotic saddle
sponsible for a globally unstable behavior known as *transient chaos* (for re
[4, 5]) which provides an example of a kind of "dynamical nonequilibriu
that cannot be understood as an asymptotic state. In such cases one
chaotic-like behavior and then, rather suddenly, a settling down to anot
which is either periodic or chaotic, but different from the transient. In othe
chaotic saddles are state space objects responsible for temporally chaotic
with finite life time. Sole investigation of the asymptotic behavior of such
would miss the interesting chaotic part contained in the transients.

Chaotic transients and chaotic saddles are common in dynamical system
are ubiquitous in *periodic windows* of bifurcation diagrams [7] in which ch
be present in the sense that there exists an infinity of unstable periodic or
their union is not attractive. Transient chaos can also be a sign for the
permanent chaos [8]. More generally, all types of *crisis* configurations [1]
companied by long chaotic transients. Large attractors born at crises inc
into themselves chaotic saddles existing before [9, 10, 11].

Chaotic saddles can also give rise to a plethora of dynamical phenome
example, if two or more periodic or chaotic attractors coexist, trajector
hesitate, possibly for a long time, to which of the attractors they asympto
attractors are typically separated by *fractal basin boundaries* [12] which ar
manifolds of chaotic saddles [13]. For scattering processes in open Hami
systems the only way that chaos can appear is in the form of transients.
scattering is then also governed by underlying chaotic saddles that now
symplectic character [14]. The passive advection of tracer particles (e.g.

dye droplets) in open hydrodynamical flows with uniform inflow and outflow velocities is one of the most appealing applications of chaotic scattering [15] - [17]. In systems subjected to external random forces, the form of attractor observed might depend on the noise intensity. The phenomenon, when a system with simple periodic attractors turns to be chaotic at sufficiently strong noise, is called *noise induced chaos* [18]. In such systems there is always a chaotic saddle coexisting with periodic attractors so that at increasing noise intensity all becomes embedded into a noisy chaotic attractor.

There is also a growing experimental evidence of motion on chaotic saddles [19] -[29]. The most detailed ones are *convection loop experiments* [20, 25], the investigation of *chemical reactions preceeding thermal equilibrium* [26], *NMR lasers* [27], and a *pendulum* experiment [28]. Recently, the first experimental investigation of chaotic scattering has been carried out in the form of chaotic tracer dynamics in the wake of a cylinder [29]. There are also every-day observations of transient chaos on finite time scale. The majority of the battery-driven chaos machines settles down to periodic motion after a typical time of no longer than one hour. The wheels of the supermarket trolleys often exhibit, even at a constant speed of towing, a shimmying motion which goes over into a smooth rolling after a while [30].

This list clearly shows the pervasiveness of transient chaos which is as a general phenomenon as stationary or permanent chaos. In fact, chaotic saddles are as robust invariant state space objects as chaotic attractors.

The rest of the Chapter is organized as follows. In Sec. 8.2, we review the basic dynamical properties of chaotic saddles. In Sec. 8.3, we present the basic idea and methodology for controlling transient chaos. In Sec. 8.4, we compare the control of transient chaos and that of sustained chaos (on attractors). In Sec. 8.5, we discuss characteristic changes in the control when a chaotic saddle is converted into a chaotic attractor, or vice versa, at a crisis. In Sec. 8.6, we present an example of controlling fractal basin boundaries. In Sec. 8.7, we describe applications to chaotic scattering. In Sec. 8.8, we discuss the idea of maintaining sustained chaotic motion in a transient chaotic regime and outline a procedure to achieve this, which can yield a high percentage of initial conditions to be controlled. The details of the algorithm are relegated to the Appendix. In Sec. 8.9, we discuss recent developments of controlling transient chaos and applications.

8.2 Properties of chaotic saddles

Chaotic saddles, similarly to chaotic attractors, contain an *infinite number* of unstable periodic orbits. They are also fractal objects. These saddles are globally *not* attracting but have a basin of attraction of zero volume in the full phase space, which is itself a fractal foliation. As an example, Fig. 8.1 shows the chaotic saddle of the Hénon map (at parameter values different from the usual ones $a = 1.4, b = 0.3$ that lead to the standard Hénon chaotic attractor.) A chaotic saddle is the chaotic analog of a saddle point which repels trajectories from its neighborhood, but has nevertheless an invariant subspace of volume zero along which it is attractive. This

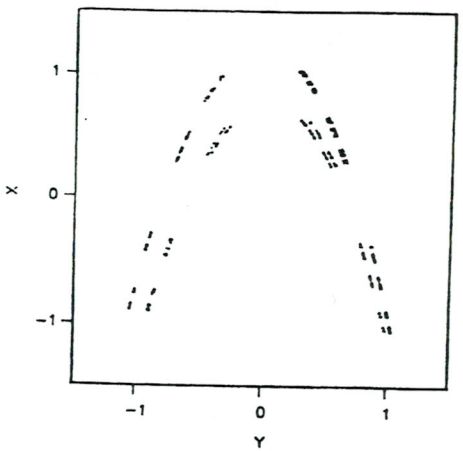

Figure 8.1 The chaotic saddle of the Hénon map $x_{n+1} = 1 - ax_n^2 + by_n, y_{n+1}$ parameters $a = 2, b = 0.3$ where no other finite invariant sets of exist. Trajectories escaping from this set go to minus infinity.

subspace is called the *stable manifold* of the chaotic saddle. The stable m provides a fractal foliation of the phase space (see Fig. 8.2). Similarly, th invariant subspace along which the chaotic set repels out those exceptiona tories that have hit it infinitely long time ago, the set's *unstable* manifol precisely, this can also be defined as the stable manifold of the time reve namics. It is worth sometimes considering the chaotic saddle as the comn of its invariant manifolds. A chaotic saddle has *more pronounced fractal pr* than a chaotic attractor. Due to the escape, the chaotic saddle has hole scales *along its unstable manifold*, too. The saddle of the Hénon map s Fig. 1 appears to be the direct product of two Cantor sets.

Chaotic saddles typically coexist in dissipative cases with an attractor Hamiltonian systems with an exit channel leading to an asymptotic motic jectories starting from randomly chosen initial points then approach the a or the asymptotic state with probability one. Because of the saddle's stab tion, however, they might come close to the saddle and stay in its vicinity fo time. What is observable numerically or experimentally is not the chaotic but rather a *small neighborhood* of it. This results in the appearance of a motion on finite time scales. The actual time spent around the saddle c sensitively on initial conditions but the average transient lifetime is typica defined.

When distributing a large number of initial points in a region contain chaotic saddle (but not the attractor(s)), trajectories emanating from these will leave the region with certainty. Those with initial points close enou branch of the stable manifold have a long time before escaping. Thus the n of points $N(n)$ staying still in the preselected neighborhood after a discre

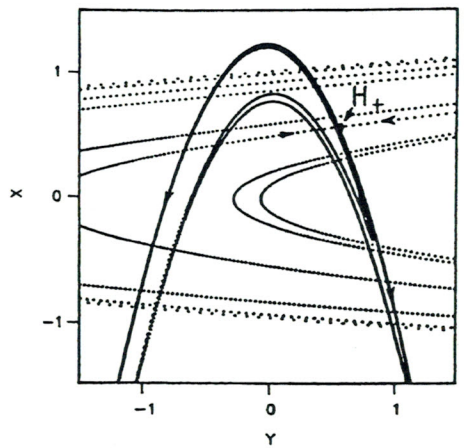

Figure 8.2 The stable (dotted lines) and unstable (full lines) manifolds of the Hénon chaotic saddle at $a = 2, b = 0.3$. H_+ represents an unstable fixed point on the saddle.

n is a function that monotonously decreases to zero. How rapidly it decreases is an important characteristics of the saddle. Often one finds that the decay is exponential for long times [2], i.e.,

$$N(n) \sim e^{-\kappa n} \tag{8.1}$$

for $n \to \infty$. The positive number κ is called the *escape rate* of the saddle and turns out to be independent of the shape of the region containing the intial points. The escape rate measures the saddle's strength of repulsion: a large escape rate marks a rather unstable saddle. Conversely, $1/\kappa$ is considered to be the average lifetime around the chaotic saddle. The case of permanent chaos is formally recovered in the limit $\kappa \to 0$.

Just as for chaotic attractors, there exist invariant distributions on chaotic saddles, too. The so-called *natural distribution* [2, 3, 4] on a saddle is obtained by distributing an ensemble of points around the set and following those with long lifetimes. The frequency of visiting different regions of the saddle by these trajectories defines the natural probability measure. One can then speak about characteristic numbers taken with respect to this measure. The average Lyapunov exponent $\overline{\lambda}$ of the saddle is of special importance since it characterizes the typical divergence of nearby trajectories staying for long times around this set. The Lyapunov exponent describes the local instability of the saddle, while the escape rate is a global measure of instability.

Numerically, chaotic saddles can be constructed with arbitrary accuracy by a technique known as the Proper-Interior-Maximum triple (PIM-triple) method [31], which is specially designed for selecting a long trajectory which is never further away from the saddle to a predefined small threshold distance value. A recent generalization of the method is able to create a trajectory which visits different parts

of the saddle according to the natural distribution [32], and thus to recon natural measure with arbitrary accuracy, too.

8.3 The basic idea for controlling chaotic s

The preceeding discussion implies that controlling the motion on chaotic a generic possibility to convert even transiently chaotic dynamics into per i.e. stabilizing one of the saddle's periodic orbits. The novel feature of th control is that it stabilizes an orbit which is *not* on the actual attractor. O thus an *atypical behavior* which cannot be seen by a long time observati unperturbed motion. One can say that this control means *stabilizing a n state.*

These general features of controlling chaotic saddles hold for any p control method applied to transient chaos. To be specific, we shall tre following the Ott-Grebogi-Yorke (OGY) method [33] because this is an a that is capable of carrying out the finest possible selection of the target be stabilized and of applying the weakest possible perturbation. Other e.g. the delayed feedback control of Pyragas [34] or the geometric contro of Toroczkai [35], are also applicable.

To achieve control by means of the OGY method, one has to use an *en* $N_0 >> 1$ trajectories [36] because any randomly chosen single initial poin with high probability to a trajectory which escapes any neighborhood of t rather quickly. This ensemble is typically chosen to start in a compa having an intersection with the saddle's stable manifold. One also selects region around a predetermined hyperbolic periodic orbit on the chaoti Then the ensemble of trajectories is started and one waits until any t enters the target region where and when the control algorithm is appli controlling perturbation is adjusted so that the predetermined periodic stabilized. Only small local perturbations are allowed, smaller in size th value δ that we call the maximum allowed perturbation. It is supposed proportional to the linear extension of the target region [33]. The actual a selecting the proper value of the perturbation parameter p_n ($\mid p_n \mid < \delta$) is the same as in the OGY control of the motion on chaotic attractors, and given in other chapters of this book. Fig. 8.3 shows a succesful control of point on the Hénon saddle in comparison with the uncontrolled traject The striking feature is that the controlled motion is not a part of the asy dynamics which is a period-5 attractor in this case. Next we summarize th behavior characterizing the ensemble in the limit of small allowed pertu $\delta << 1$. Many of the trajectories escape this region before they can enter th region selected around a periodic orbit on the chaotic saddle. Short transi therefore irrelevant for the controlling process, while very long ones are un find. It is thus qualitatively clear that the average time τ needed to achieve is independent of δ and is limited from above by the chaotic lifetime $1/\kappa$ w

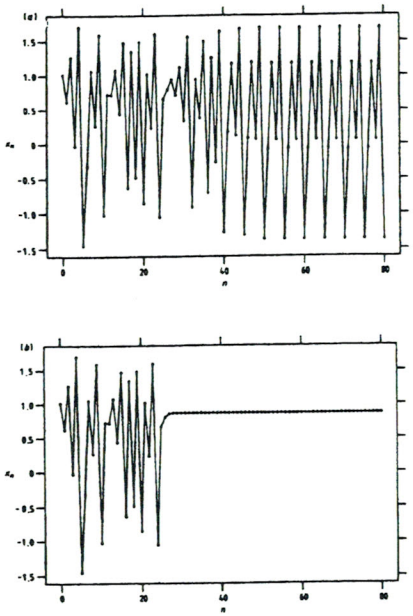

Figure 8.3 (a) Transient chaotic signal x_n versus n starting from the point $x_0 = y_0 = 1.014782$ in the Hénon map at parameters $a = 1.45, b = 0.3$ where the attractor is a period-5 cycle. The trajectory ceases to be chaotic at about the 38th time step where it comes to the neighbourhood of the periodic attractor. (The average lifetime of chaotic transients is $1/\kappa = 22$ at these parameters.) (b) Controlled signal started from the same initial point. The Hénon map was taken in the form given in the caption to Fig. 0.1 with $a = 1.45 + p_n$ where the maximum allowed perturbation in $\mid p_n \mid$ is $\delta = 0.1$. The fixed point is at $x_F = y_F = 0.868858$. Control sets in at the 26th step and the fixed point on the saddle becomes stabilized.

maximum allowed control δ goes to zero:

$$\tau(\delta) = \text{independent of } \delta \leq 1/\kappa. \tag{8.2}$$

Because of escape, only a small portion of all trajectories can be controlled. Moreover, the number of controlled trajectories $N(\delta)$ has been found [36] to decrease with decreasing δ according to a power law:

$$N(\delta) \sim \delta^{\gamma(\kappa)} \tag{8.3}$$

where the exponent $\gamma(\kappa)$ depends on the escape rate, too.

In the particular case when the target region is a ball around a fixed point of a two-dimensional map, the exponent $\gamma(\kappa)$ characterizing the decay of the number

of controlled trajectories is [36]

$$\gamma(\kappa) = 1 + \frac{\ln \mid \lambda^{(u)} \mid - \kappa}{\ln \mid 1/\lambda^{(s)} \mid},$$

with $\lambda^{(s)}$ and $\lambda^{(u)}$ as the eigenvalues of the fixed point to be stabilized.

8.4 Comparison with controlling perm chaos

When applying the OGY method to controlling permanent chaos, the sca erties of an ensemble of N_0 trajectories are different. The average time τ achieve control is a function of the linear size of the target region which is to be proportional to the maximum allowed perturbation δ during cont been pointed out [33] that $\tau(\delta)$ increases as a power of δ when δ tends to

$$\tau(\delta) \sim \delta^{-\gamma},$$

where $\gamma > 0$ is a characteristic exponent. This scaling law, which s the dynamics of reaching the target region is itself a kind of transient recently been verified experimentally [37]. On the other hand, the numb controlled trajectories does not depend on δ:

$$N(\delta) = N_0$$

since all of the N_0 trajectories of the ensemble are controlled sooner or

Thus, the shown scaling behavior in the control of permanent and chaos appear to be the two extremes of a general process (in the first ca constant, while in the second $\tau(\delta)$). Interestingly, there exists a unifyir between $N(\delta)$ and $\tau(\delta)$ which holds in both cases [38]. The key observat the number of controlled trajectories in the entire process is proportio average number of trajectories controlled *per unit time* multiplied by tl time needed to achieve control. The average number of trajectories con time step is proportional to the probability to fall in the target regic some measure $\mu(\delta)$ of the target region. The measure μ to be taken for I and transient chaos is the *natural measure* of the attractor and the *co invariant measure* of the nonattracting chaotic set, respectively. The la probability that trajectories which have not yet escaped a given neighbc the chaotic set fall into the target region [39, 4]. Thus we can write

$$N(\delta) \sim \mu(\delta)\tau(\delta).$$

This relation contains as special cases Eqs. (8.3,8.6) (for τ =const and for respectively), and shows that the exponents γ of (8.5) and $\gamma(\kappa)$ of (8.3) a the scaling law of $\mu(\delta)$:

$$\mu(\delta) \sim \delta^{\gamma(\kappa)}.$$

Since for permanent chaos $\kappa = 0$,

$$\gamma = \gamma(\kappa = 0) \tag{8.9}$$

must also hold.

As an important consequence of Eq. (8.8), the number $\varrho(\delta)$ of trajectories controlled per time steps follows a simple scaling law:

$$\varrho(\delta) \equiv \frac{N(\delta)}{\tau(\delta)} \sim \delta^{\gamma(\kappa)}, \tag{8.10}$$

and this is valid in both permanent ($\kappa = 0$) and transient ($\kappa > 0$) chaotic cases.

8.5 Crossover around crises

The essential difference between the scaling of $N(\delta)$ and $\tau(\delta)$ of the controlling process for permanent and transient chaos can only be explained by the fact that the limits $\delta \to 0$ and $\kappa \to 0$ are *not* interchangable. There must, therefore, exist a crossover from Eq. (8.2) to Eq. (8.5) (and from Eq. (8.3) to Eq. (8.6)) as κ goes to zero.

The phenomenon of diminishing escape rate, i.e., diverging chaotic life-time, can always be observed when a nonlinearity parameter a decreases in the transient chaotic region and tends to a critical value a_c marking the crisis value where permanent chaos first sets in. The dependence of the escape rate on a has been found [9] to follow a power-law in $(a - a_c)$:

$$\kappa(a) = C(a - a_c)^{\tilde{\gamma}} \tag{8.11}$$

with a positive $\tilde{\gamma}$ as $a \to a_c$.

In the range of small values of δ and $a - a_c > 0$, there are two time-scales which at suitable choices of a and δ might be of the same order of magnitude: the average lifetime of chaos at parameter a, $1/\kappa(a)$, and the average time needed to achieve control $\tau(\delta, a_c) \sim \delta^{-\gamma(0)}$ at the crisis point. Thus one expects that the average time $\tau(\delta, a)$ needed to achieve control for $(a - a_c)/a_c << 1$ follows a *scaling law*:

$$\tau(\delta, a) = \tau(\delta, a_c) f[\kappa(a)\tau(\delta, a_c)] \tag{8.12}$$

where the *scaling function* $f(x)$ depends on the dimensionless variable product $\kappa(a)\tau(\delta, a_c)$ only. In fact, $f(x)$ must tend to one as $x \to 0$ and must be inversely proportional to x as $x \to \infty$.

It is easy to derive [38] that the scaling function has the explicit form

$$f(x) = (1 + x)^{-1} \tag{8.13}$$

which is a mean-field-type result.

¿From this the rules Eqs. (8.2,8.3) and (8.5,8.6) are recovered for $\delta \to 0$ at a fixed (when $\tau(\delta, a_c) \to \infty$, and $f(x) \to 1/x$) and for $a \to a_c$ at δ fixed (when

$\kappa(a) \to 0$ and $f(x) \to 1$), respectively. A crossover between these behav
place when the two characteristic times are of the same order of magnitu

$$\tau(\delta, a_c)\kappa(a) \approx 1.$$

The crossover region is typically rather narrow because of the small values
[38]. Therefore, it is unlikely to numerically find the crossover behavior, c
sees the scaling (8.2,8.3) valid for chaotic saddles or (8.5,8.6) valid for attr
is, however, important to know that between these drastically different l
there is a smooth interpolation.

8.6 Controlling motion on fractal basin b aries

An immediate application of the control of chaotic saddles is the control o
tion on fractal basin boundaries [40], which in physical systems typically
chaotic saddle whose stable manifold is the boundary [12]. One can then s
periodic cycles of the saddle to control. By applying the method sketche
a hyperbolic orbit hesitating to go to any of the attractors, (a Balam's d
converted into an attracting orbit by applying weak perturbations.

Figure 8.4 shows a continuous-time example, the case of a driven dam
dulum. At the parameter set investigated there are two attractors, ea
sponds to a periodic winding motion (interrupted by a swinging), whose
attraction is bounded by a fractal curve in the phase space. A period-1
motion is selected as the motion to be stabilized on the chaotic saddle s
the basin boundary. The OGY control algorithm is applied at integer
of the driving period, i.e. on the stroboscopic map of the system, by ma
driving amplitude slightly time-dependent. The upper part of Fig. 8.4 e
successful control process leading to the stabilization of a periodic motion
basically different from *any* of the two periodic attractors.

This method is potentially important in applications where periodic
can result in a catastrophic failure of the system. A particular exampl
ship capsizing. The method of controlling motion on fractal basin bound
succesfully been extended to preventing chaos-induced ship capsizing even
when the driving due to environmental influences (e.g. waves) is not peri
has substantial irregular (chaotic) component [41].

8.7 Controlling chaotic scattering

A novel feature of chaotic saddles in Hamiltonian systems is that they t
also have a *nonhyperbolic component* where the local Lyapunov exponent
be arbitrarily close to zero. An interesting question is therefore to investi
influence of the nonhyperbolic component on the control process. The hy
component has a similar direct product Cantor set structure as shown

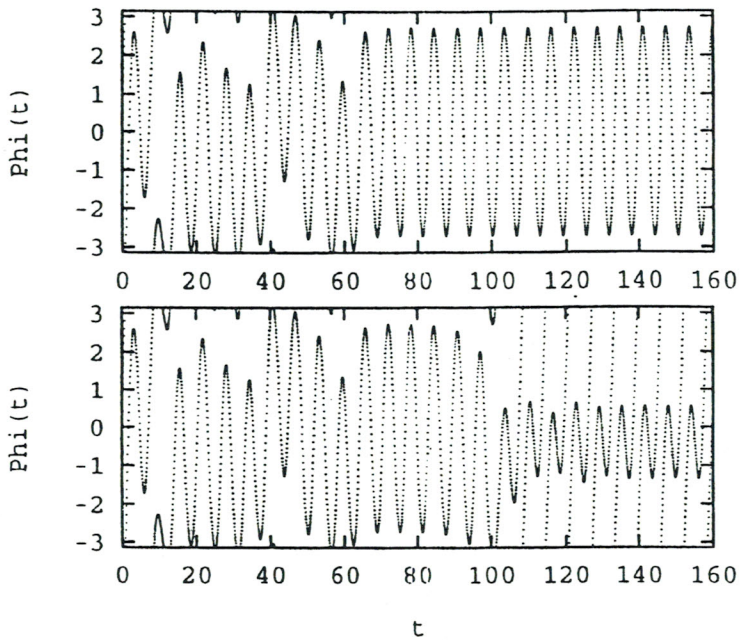

Figure 8.4 (a) Time dependence of the angle $\Phi(t)$ of the driven pendulum $\ddot{\Phi} + \beta\dot{\Phi} + sin\Phi = \rho(t)\ \cos\omega t$ with $\rho(t) = \rho_0 + \varrho(t)$ started from $\Phi_0 = 0.5806$, $\dot{\Phi}_0 = 2.7524$ at $t = 0$. The parameters are $\beta = 0.2, \omega = 1$, $\rho_0 = 2$. The trajectory enters the target region, a disk of radius 0.05 around the unstable fixed point $(-2.6313, 0.6516)$ on the stroboscopic map talen at $t = 0$ mod $2\pi/\omega$. After 10 driving cycles control sets in, $\varrho(t)$ is chosen to cause the pendulum to keep swinging without rotation, i.e., to remain on the basin boundary (upper panel). Without control, $\varrho(t) \equiv 0$ (lower panel), the same trajectory is attracted to a stable winding motion (interrupted by swinging).

8.1 just more symmetric since, because of the time reversal invariance, the stable and unstable manifolds are equivalent. The stabilization of periodic orbits on the hyperbolic component is therefore similar to that discussed in Sec. 8.3. The nonhyerpbolic component is close to the KAM surfaces surrrounding quasiperiodic islands. If one selects a periodic orbit close to such a KAM surface, the time to achieve control is obviously long due to the stickiness of these surfaces. Numerical investigation shows [42] that the average time to achieve control could be an order of magnitude longer than the average chaotic lifetime on the hyperbolic component. The details of the actual behavior might depend on the inital condition of the ensemble investigated. Anyhow, Eq. (8.2) is no longer valid, but τ seems to be still limited from above when the maximum allowed perturbation goes to zero. This is illustrated by the numerically obtained distribution of the average times

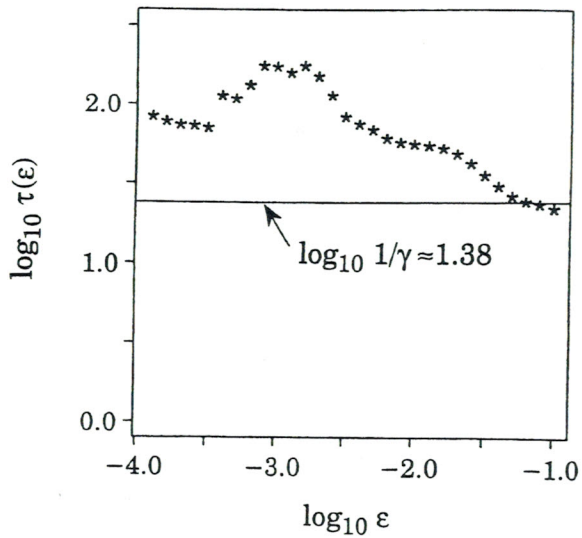

Figure 8.5 The average time $\tau(\epsilon)$ to achieve control in a chaotic scattering sy for an ensemble of trajectories visiting the nonhyperbolic compon saddle before being captured on a peridic orbit. It is given as a fu the linear size ϵ of the target region which is proportional to the r allowed perturbation, δ. The straight line marks the reciprocal va escape rate, the average control time on the hyperbolic compoene that $\tau(\epsilon)$ greatly exceeds this for small sized target regions.

to achieve control shown in Fig. 8.5 which holds for trajectories comin vicinity of a KAM torus, i.e., moving on the nonhyperbolic componen being controlled. The number of controlled trajectories scales accordin (8.3) since this number depends only on the probability to hit the targe no matter how long it takes for the individual trajectories to enter thi Generally speaking, controlling a collisional scattering process means *stabil intermediate complexes* of a reaction which would otherwise be of finite l The findings mentioned above show that although the effect of KAM surf be important for the controlling process, the qualitative behavior of the c ensemble is similar to that of fully hyperbolic systems.

8.8 An improved control of chaotic saddles

As we discussed in Sec. 8.4, a major difference between stabilizing unstable orbits embedded in a chaotic attractor and a chaotic saddle is that for the attractor, the probability that a chaotic trajectory enters the neighborhoc

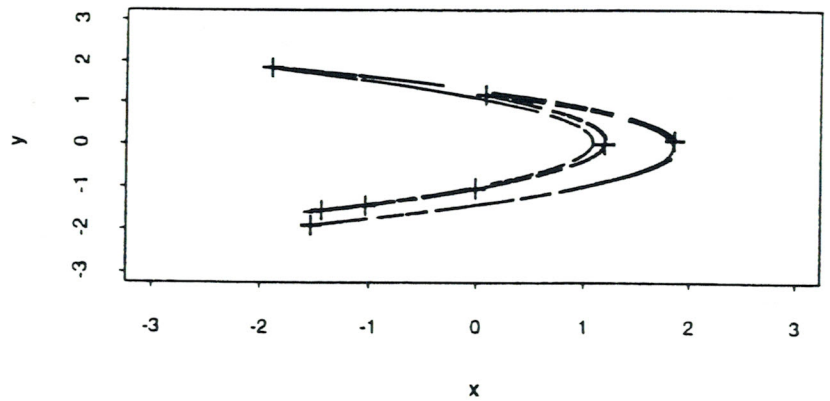

Figure 8.6 A chaotic saddle for the Hénon map $x_{n+1} = a - x_n^2 + by_n, y_{n+1} = x_n$ at $a = 1.5$, $b = 0.3$. The crosses denote the locations of a period-8 orbit embedded in the chaotic saddle.

desired unstable periodic orbit is one [33]. Hence, trajectories originating from almost any initial condition in the basin of the chaotic attractor can eventually be stabilized. While for the case of transient chaos, only a small set of initial conditions can be controlled. The reason is that most trajectories will have already left the chaotic saddle before entering the neighborhood of the target periodic orbit. A possible remedy is to simultaneously launch an ensemble of initial conditions and to control any one of the trajectories that come close to the target periodic orbit as demonstrated in Sec. 8.3. Clearly, for transient chaos we can only talk about the probability that a randomly chosen initial condition can be controlled. This probability is usually very small [36]. The main objective of this Sec. is to describe a scheme that can be utilized to maximize this probability.

The key observation is that there exists a dense chaotic orbit on the chaotic saddle (the complement of the set of all unstable periodic orbits on the saddle) *that comes arbitrarily close to any target unstable periodic orbit*, as shown in Fig. 8.6 for a chaotic saddle of the Hénon map. By using the PIM-triple method [31], one can compute such a long *reference orbit* on the chaotic saddle. The probability that a trajectory approaches this reference orbit is greater than the probability that this same trajectory enters the neighborhood of the target unstable periodic orbit before it escapes, if the length of the reference orbit is long enough. By *stabilizing a trajectory around the reference orbit first, and then switching to stabilize it around the target periodic orbit after the trajectory comes close to the periodic orbit*, we

can *substantially* increase the probability that a trajectory can be contro can indeed be achieved since there exist stable and unstable direction point of the reference orbit on the chaotic saddle. Hence, in principle, c a trajectory near the reference orbit is equivalent to stabilizing a long periodic orbit as in Ref. [33]. The longer the length of the reference orl larger the probability for controlling periodic orbits can be.

Our idea of control is as follows [43]. Let $\mathbf{x}_{n+1} = \mathbf{F}(\mathbf{x}_n, p)$ be a two-di invertible map that exhibits transient chaos. Let $\{\mathbf{y}_n\}$ $(n = 0, 1, 2, \ldots, N)$ long reference orbit on the chaotic saddle obtained by the PIM-triple me Now generate the orbit $\{\mathbf{x}_n\}$ to be stabilized around the reference orbit. F pick an initial condition $\mathbf{x}_0$, assume that the orbit point $\mathbf{x}_n$ $(n \geq 0)$ falls i neighborhood of the point $\mathbf{y}_k$ of the reference orbit on the chaotic saddl step n. Without loss of generality, we set $k = n$ on the reference orbit small neighborhood, the linearization of $\mathbf{F}$ is applicable. We have, thus,

$$\mathbf{x}_{n+1}(p_n) - \mathbf{y}_{n+1}(p_0) = \mathbf{J} \cdot [\mathbf{x}_n(p_0) - \mathbf{y}_n(p_0)] + \mathbf{K}\Delta p_n,$$

where $\Delta p_n = p_n - p_0$, $\Delta p_n \leq \delta$, $\mathbf{J}$ is the 2×2 Jacobian matrix an two-dimensional column vector,

$$\mathbf{J} = \mathbf{D_X F}(\mathbf{x}, p)|_{\mathbf{x}=\mathbf{y}_n, p=p_0}, \quad \mathbf{K} = \mathbf{D}_p \mathbf{F}(\mathbf{x}, p)|_{\mathbf{x}=\mathbf{y}_n, p=p_0}.$$

Without control, *i.e.*, $\Delta p_n = 0$, the orbit $\mathbf{x}_i$ $(i = n+1, \ldots)$ diverges fron erence orbit $\mathbf{y}_i$ $(i = n+1, \ldots)$ exponentially. Our task is to program the p perturbations Δp_n in such a way that the trajectory $\mathbf{x}$ stays near the orbit on the chaotic saddle (or equivalently, $|\mathbf{x}_i - \mathbf{y}_i| \to 0|$) for subsequen $i \geq n + 1$.

For each reference orbit point on the chaotic saddle, there exist both and an unstable direction. (For higher dimensional maps, there may b stable and unstable directions. The algorithm to control chaos in such more complicated [44] and will not be discussed here.) The existence of t and unstable directions at each reference orbit point can be seen as follow choose a small circle of radius ε around some orbit point $\mathbf{y}_n$ and map t to $\mathbf{y}_{n-1}$ by the inverse map. In a Cartesian coordinate system with the $\mathbf{y}_{n-1}$, the deformed circle can be expressed as $A(dx')^2 + B(dx')(dy') + C($ which is typically an ellipse. Here A, B and C are functions of the entri inverse Jacobian matrix at $\mathbf{y}_n$. This deformation from a circle to an ellip that distance along the major axis of the ellipse at $\mathbf{y}_{n-1}$ contracts as a res map. Similarly, the image of a circle at $\mathbf{y}_{n-1}$ under $\mathbf{F}$ is typically an ellip which means that distance along the inverse image of the major axis of tl at $\mathbf{y}_n$ expands under $\mathbf{F}$. Thus the major axis of the ellipse at $\mathbf{y}_{n-1}$ and th image of the major axis of the ellipse at $\mathbf{y}_n$ approximate the stable and directions at $\mathbf{y}_{n-1}$. It should be noted that, typically, the stable and directions are not orthogonal to each other. In nonhyperbolic chaotic syst can even coincide [45].

To achieve control, it is neccessary to calculate the stable and unstat tions along the reference orbit. We use an algorithm developed in Ref. [4

numerical method, however, requires that the Jacobian matrix of the map be explicitly known. The stable and unstable directions are then stored together with the reference orbit, and they are used to compute the parameter perturbations applied at each time step. The details of the algorithm are given in the Appendix.

We now present a numerical example. Figures 8.7(a-b) show an example of applying our algorithm to the chaotic saddle of the Hénon map at $a = 1.5$ and $b = 0.3$. We use a reference orbit on the chaotic saddle of length $N = 10000$. The maximally allowed parameter perturbation is $\delta = 0.01$ and the size of the small neighborhood around each point on the reference orbit is chosen to be $\epsilon = 0.005$. We can choose both δ and ϵ arbitrarily, as long as they are small. We start the trajectory to be stabilized with initial condition: $(x_0, y_0) = (0.5, -0.1)$. After 4 initial iterates, the trajectory falls into the neighborhood of a point of the reference orbit $[(x, y) \approx (-1.8393, 1.8387)]$. When this occurs, parameter control based on Eq. (8.18) is turned on to stabilize the trajectory around the reference orbit. At the time step $n = 846$, the controlled chaotic trajectory comes into the vicinity of the period-8 orbit, at which time we immediately turn on a new set of parameter perturbations calculated with respect to the period-8 orbit. The trajectory stays in the neighborhood of the period-8 orbit in subsequent iterations as long as the parameter perturbation is present. Figure 8.7(b) shows values of the parameter perturbations applied. Numerically, the controlled trajectory rapidly converges to the reference orbit both after $n = 4$ (stabilized around the reference orbit) and after $n = 846$ (stabilized around the period-8 orbit). After a few iterates, the parameter perturbations required become extremely small (around 10^{-10}). The probability that a randomly chosen initial condition can be controlled, $P(N, \epsilon)$, depends both on the length of the reference orbit N and the size ϵ of the small region around each reference point. Figure 8.8(a) shows the $P(N, \epsilon)$ versus N curve, where $\epsilon = 0.005$. This curve is calculated by varying N systematically and randomly choosing 10^4 initial conditions with uniform probability distribution in the square region of Fig.. 8.6 for each fixed N value. The probability is given by the ratio between the number of initial conditions that approach the reference orbit before escaping to infinity and the total number of initial conditions chosen (10^4). For small N values, say $N < 800$, $P(N, \epsilon)$ increases approximately linearly. The reason is that the probability that a trajectory enters the neighborhood of the chaotic saddle is approximately proportional to the total area of the small circles surrounding all the reference orbit points. This area is approximately $\pi\epsilon^2 N$ when overlaps between neighboring circles are small. As N increases further, the overlaps between neighboring circles become significant, thereby causing $P(N, \epsilon)$ to saturate. In fact, when $N > 1000$, $P(N, \epsilon)$ increases very slowly. For $N = 1000$, $P(N, \epsilon) = 0.546$. For $N > 10000$, we have $P(N, \epsilon) > 0.66$. We expect the optimal length of the reference orbit to be $N \sim 1/\epsilon$, the point when overlap starts to become significant. If a trajectory is directly stabilized around the period-8 orbit without being stabilized around the reference orbit, the probability that an initial condition can be controlled is *only 0.04* as shown by the lower straight line in Fig. 8.8(a). Thus, *by using a reference orbit of length about* 1000, *a factor of more than 10 improvement in this probability*

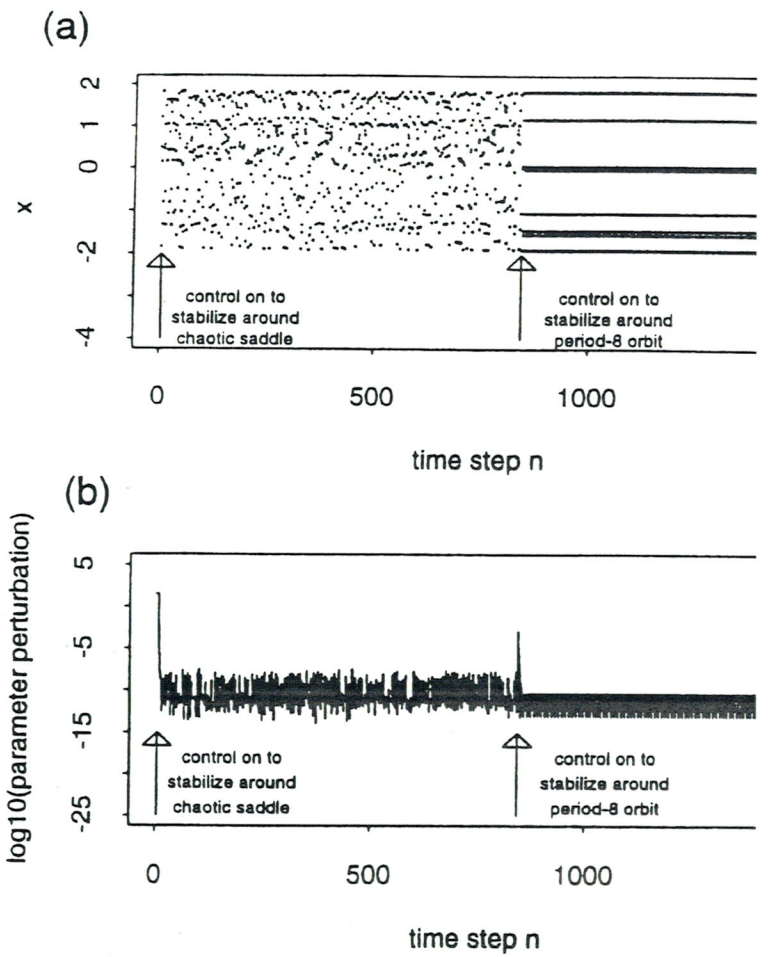

Figure 8.7 (a) An example of stabilizing the unstable period-8 orbit shown in F means of the improved control method. A trajectory starts with condition $(x_0, y_0) = (0.5, -0.1)$. At time step $n = 4$, it falls in a neig of one point on the reference orbit. Parameter control is turned on t the trajectory around the reference orbit for $n \geq 4$. At $n = 846$, the chaotic trajectory gets close to the period-8 orbit. A new set of p perturbations calculated with respect to the period-8 orbit is tur stabilize the trajectory. For $n \geq 846$, the controlled motion is peri The time-dependent parameter perturbations applied at each time

can be achieved. The relation between $P(N, \epsilon)$ and ϵ for fixed $N = 8000$ is shown by the upper curve in Fig. 8.8(b). As a contrast, the lower curve in Fig. 8.8(b) shows the same probability when no reference orbit is used to stabilize the period-8 orbit.

Remarks:

(a) The above method can also be applied to convert transient chaos into sustained chaos [46]. By constructing an arbitrarily long reference orbit on the chaotic saddle, we can make other trajectories stay in the neighborhood of this reference orbit for as long as we wish by applying small parameter control. In this sense, non-attracting trajectories in the neighborhood of the chaotic saddle are transformed into stable chaotic trajectories.

(b) In a similar way, a method for stabilizing chaotic orbits on the attractor has been proposed and applied to the synchronization of two almost identical chaotic systems [47], and a method of creating desired chaotic orbits on a chaotic attractor has been implemented [48].

8.9 Discussions

In this Chapter we review the basic problem of controlling transient chaos on chaotic saddles. Through the use of scaling relations, we compare controlling transient chaos with the more extensively studied problem of controlling permanent chaos on chaotic attractors. Below we discuss several applications.

Controlling transient chaos may have applications to engineering (*e.g.*, the voltage-collapse problem [49]) and ecology (*e.g.*, the species extinction problem [50]). In electrical engineering, in a particular type of voltage collapse, the power supply system suddenly breaks down after exhibiting complicated dynamical behavior resembling that of transient chaos. Theoretical models for this type of voltage collapse suggest that transient chaos may be the culprit [49]. Therefore, the conversion of a transient chaotic trajectory into a sustained chaotic or periodic trajectory would prevent the voltage collapse. In ecology, in certain situations the problem of species extinction can be addressed using the idea of transient chaos [50]. Specifically, it was recently suggested by McCann and Yodzis [50] that transient chaos in very simple but biologically reasonable ecosystem models, mathematically described by coupled ordinary differential equations, can provide a hint as to how local species extinction can arise without the necessity to consider temporal or spatial variations and external factors. Usually, the population size of some species can behave chaotically for a (long) period of time and then decreases to zero in a relatively short period of time. Our idea is that if species extinction is caused by transient chaos, then it is possible for human being to intervene externally by applying perturbations so as to effectively prevent species from becoming extinct. The magnitude of the applied perturbation can be made arbitrarily small, and the perturbations need to be applied only occasionally. As such, the natural dynamics of the species population is hardly influenced, and yet, the population, though still exhibiting chaotic behavior, will never become zero. The implication is that in a

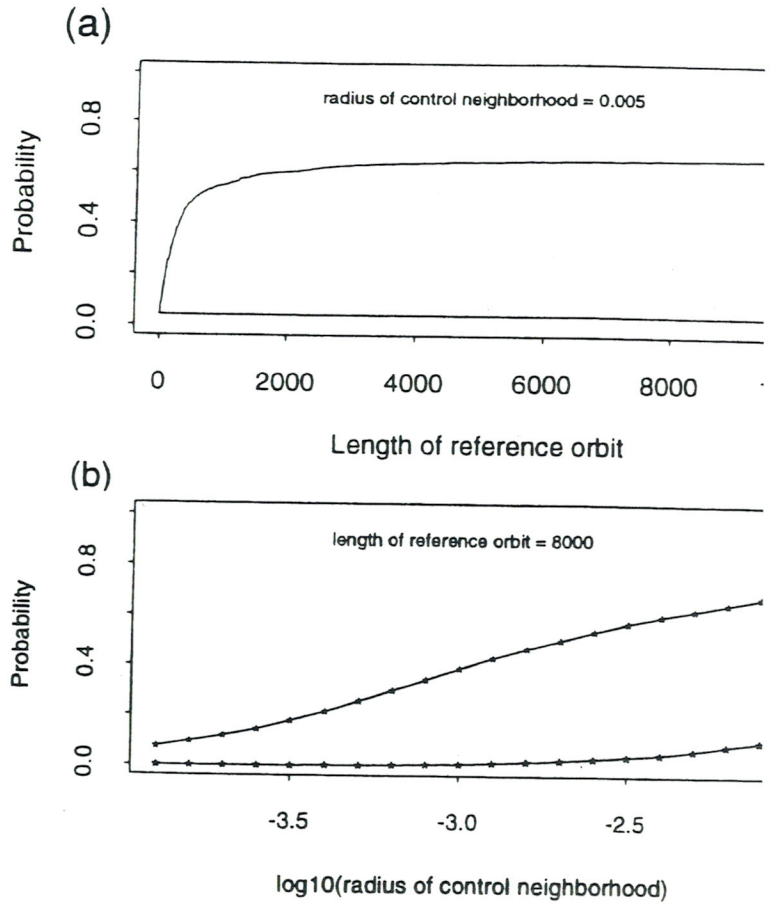

Figure 8.8 (a) For fixed $\epsilon = 0.005$ (the radius that defines the controlling n hood), the probability $P(N, \epsilon)$ that a randomly chosen initial condi be controlled versus N, the length of the reference orbit (the uppe This probability increases initially with N and saturates for large asymptotic value of $P(N, \epsilon)$ is approximately 0.66. The lower stra represents the probability that the trajectory is directly stabilized ar period-8 orbit. The value of this probability is only 0.04. Therefore, a reference orbit of length about 1000, a factor of more than 10 impr in this probability can be achieved. (b) For fixed $N = 8000$, $P(N, \epsilon)$ curve (upper curve). The lower curve is the same probability versus the trajectory is directly stabilized around the period-8 orbit.

realistic ecological environment, a very small amount of artificially imposed change to population sizes or some small disturbance to the environment, only very rarely applied, can prevent species extinction over long time scales. Potentially, this can be of paramount interest to the significant and growing environmental problem of species preservation. A strategy for controlling transient chaos based on time series with applications to the voltage-collapse and species-extinction problems was recently studied [51].

Controlling transient chaos also has applications to nonlinear digital communication. Previous work demonstrated that symbolic representations of controlled chaotic orbits could be utilized for digital communication [52]. A central issue in any digital communication device concerns with the *channel capacity*, a quantity that measures the amount of information that the device can encode. It is thus highly desirable to have the channel capacity as large as possible to maximize the amount of information that can be encoded. For a chaotic system, channel capacity is equivalent to the *topological entropy* because it defines the rate at which information is generated by the system. Recently, it was pointed out that it is generally more advantageous to use *transient chaos naturally arising in wide parameter regimes of nonlinear systems* as information sources from the standpoint of channel capacity [53]. This is based on the observation that, typically, the orbital complexity associated with trajectories on a chaotic saddle can be greater than that of trajectories on a chaotic attractor. Thus, transient chaos can yield larger channel capacity. Thus, it is highly desirable to design a chaotic system operating in a transient chaotic regime for digital communication. In Ref. [53], a procedure was proposed for encoding digital messages into trajectories that live on chaotic saddles and, it was also argued that digital encoding with chaotic saddles can be robust against environmental noise, thereby significantly reducing the probability of bit error in communication.

Another promising application is based on controlling point vortices in ideal fluids around an obstacle by means of an OGY-type control. In open flows this corresponds to the class of problems we have investigated. The surprising outcome is, however, that the viscous problem, in which one can speak of smooth vorticity ditributions instead of singular point vortices, can also be controlled practically with the same strategy as the point vortex problem. This has been poined out by Kadtke, Péntek, and Pedrizzetti [54] who developed a numerical method to stabilize a finite, concentrated vortex around a rotating cylindrical body embedded in an open fluid flow. As control parameter they used both the rotation frequency of the cylinder and the background flow velocity. The control algorithm is based on a low-dimensional Hamiltonian point vortex model, which is practically a scattering problem. This is the first example to control transient dynamics of spatially extended systems based on low-dimensional approximate dynamics. In a practical sense, the method has important consequences for any problem with vortex-body interactions, like e.g., the interaction of atmospheric vortex rings with aircraft wings where it can reduce the chance for a sudden decrease of the lift.

A further practical application of controlling motion on chaotic saddl a semiconductor double heterostructure in which the electric currents w to exhibit transiently chaotic dynamics in a wide range of parameters. dimensional model is was demonstrated by Reznik and Schöll [55] that tinuous delayed feedback method [34] can succesfully be used to stabilize periodic motions on the saddle. This opens the possibility to create this w tunable self oscillators which might be of practical relevance.

Very recently even experimental realizations of the control of transi have been reported by Kopp [56]. The motion on the chaotic saddle of t scroll circuit as well as of an electrochemical reaction have been controlled time series observation and the delayed feedback method. This illustrates trolling transient chaos in laboratories is feasible, and it will hopefully be be several other experiments.

Acknowledgments

We would like to thank the enjoyable and fruitful collaboration with C. Jung, Z. Kovács, Á. Péntek, K. G. Szabó, and Z. Toroczkai. This supported by the Hungarian National Science Foundation grants T019483 US-Hungarian Joint Fund No.286, 501.

Appendix: The improved control algorithm

To find the stable direction at a point $\mathbf{y}$, we first iterate this point forward under the map $\mathbf{F}$ and get a trajectory $\mathbf{F}^1(\mathbf{y})$, $\mathbf{F}^2(\mathbf{y})$, ..., $\mathbf{F}^N(\mathbf{y})$. Now im put a circle of arbitrarily small radius ε at the point $\mathbf{F}^N(\mathbf{y})$. If we iterate t backward once, the circle becomes an ellipse at the point $\mathbf{F}^{N-1}(\mathbf{y})$ with t axis along the stable direction of the point $\mathbf{F}^{N-1}(\mathbf{y})$. We continue itera ellipse backwards, while at the same time normalizing the ellipse's majo be of the order ε. When we iterate the ellipse all the way back to the poi ellipse becomes very thin with its major axis along the stable direction at if N is large enough. It should be mentioned that this same method ca used to compute the stable and unstable directions along unstable periodi For an unstable period-k orbit, we choose $N = mk$ so that N is large, is an integer. In practice, instead of using a small circle, we take a un at the point $\mathbf{F}^N(\mathbf{y})$ since the Jacobian matrix of the *inverse map* $\mathbf{F}^{-1}$ vector in the tangent space of $\mathbf{F}$ towards the stable direction. Thus, we unit vector backward to the point $\mathbf{y}$ by multiplying by the Jacobian matr inverse map at each point on the *already existing* orbit. We normalize th after each multiplication to the unit length. For sufficiently large N, vector so obtained at $\mathbf{y}$ is a good approximation of the stable direction at point in the calculation is that we do *not* actually calculate the inverse matrix along the trajectory *by* iterating the point $\mathbf{F}^N(\mathbf{y})$ backwards u

inverse map $\mathbf{F}^{-1}$. The reason is that if we do so, the trajectory will usually diverge from the original trajectory $\mathbf{F}^N(\mathbf{y})$, $\mathbf{F}^{N-1}(\mathbf{y})$, ..., $\mathbf{F}^1(\mathbf{y})$ after only a few backward interations. What we do is to store the inverse Jacobian matrix at every point of the orbit $\mathbf{F}^i(\mathbf{y})$ $(i = 1, \ldots, N)$ when we iterate forward the point $\mathbf{y}$ beforehand.

Similarly, to find the unstable direction at point $\mathbf{y}$, we first iterate $\mathbf{y}$ backward under the inverse map N times to get a backward orbit $\mathbf{F}^{-j}(\mathbf{y})$ with $j = N, \ldots, 1$. We then choose a unit vector at point $\mathbf{F}^{-N}(\mathbf{y})$ and iterate this unit vector forward by multiplying by the Jacobian matrices. The final vector at point $\mathbf{y}$ is a good approximation of the unstable direction at that point if N is large enough. Again, to avoid divergence from the original trajectory, we do not actually iterate the inverse map. What we do in this case is to choose $\mathbf{y}$ to be the end point of a forward orbit, all the points before $\mathbf{y}$ are the inverse images of $\mathbf{y}$ and we store the Jacobian matrix of forward map at those points.

The method so described is efficient. For instance, the error between the calculated and real stable or unstable directions is on the order of 10^{-10} for chaotic saddles in the Hénon map if $N = 20$ [45].

Let $\mathbf{e}_{s(n)}$ and $\mathbf{e}_{u(n)}$ be the stable and unstable unit vectors at $\mathbf{y}_n$ and, $\mathbf{f}_{s(n)}$ and $\mathbf{f}_{u(n)}$ be the corresponding unit contravariant vectors that satisfy $\mathbf{f}_{u(n)} \cdot \mathbf{e}_{u(n)} = \mathbf{f}_{s(n)} \cdot \mathbf{e}_{s(n)} = 1$ and $\mathbf{f}_{u(n)} \cdot \mathbf{e}_{s(n)} = \mathbf{f}_{s(n)} \cdot \mathbf{e}_{u(n)} = 0$. To stabilize $\{\mathbf{x}_n\}$ around $\{\mathbf{y}_n\}$, we require the next iteration of $\mathbf{x}_n$, after falling into a small neighborhood around $\mathbf{y}_n$, to lie on the stable direction at $\mathbf{y}_{(n+1)}(p_0)$, *i.e.*,

$$[\mathbf{x}_{n+1} - \mathbf{y}_{(n+1)}(p_0)] \cdot \mathbf{f}_{u(n+1)} = 0. \tag{8.17}$$

Substituting Eq. (8.15) into Eq. (8.17), we obtain the following expression for the parameter perturbation,

$$\Delta p_n = \frac{\{\mathbf{J} \cdot [\mathbf{x}_n - \mathbf{y}_n(p_0)]\} \cdot \mathbf{f}_{u(n+1)}}{-\mathbf{K} \cdot \mathbf{f}_{u(n+1)}}. \tag{8.18}$$

It is understood in Eq. (8.18) that if $\Delta p_n > \delta$, we set $\Delta p_n = 0$.

After a trajectory is stabilized around the reference orbit, we monitor the trajectory to see if it gets close to the target periodic orbit. To guarantee that the trajectory will always approach the target periodic orbit at later times, a possible strategy is to let the end point of the long reference orbit be in the neighborhood of the target periodic orbit. As soon as the controlled chaotic trajectory is in the vicinity of the target periodic orbit, a new set of parameter perturbations computed with respect to the periodic orbit is turned on to stabilize the trajectory around it. The new parameter perturbations can be computed similarly [Eq. (8.18)], except that the stable, unstable and their corresponding contravariant vectors are now associated with the target periodic orbit. These directions can be calculated using the same method discussed above [57].

References

[1] C. Grebogi, E. Ott and J. Yorke, Phys. Rev. Lett. **48**, 1507 (1982); Physica D **7**, 181 (1983).

[2] H. Kantz and P. Grassberger, Physica **D 17**, 75 (1985).

[3] G. H. Hsu, E. Ott, and C. Grebogi, Phys. Lett. **127A**, 199 (1988).

[4] T. Tél, Transient chaos, in *Directions in Chaos*, Vol.3, ed.: Bai-lin Ha Scientific, Singapore, 1990) pp. 149-221

[5] T. Tél, Transient chaos: a ype of metastable state, in *STATPHY* Bai-lin Hao (World Scientific, Singapore, 1996) pp. 346-362

[6] B. R. Hunt, E. Ott, and J. A. Yorke, Phys. Rev. **E54**, 4819 (1996)

[7] Y. Yorke et al., Phys. Rev. Lett. **54**, 1095 (1985)).

[8] J. A. Yorke and E. D. Yorke, J. Stat. Phys. **21**, 263 (1979).

[9] C. Grebogi, E. Ott, and J. Yorke, Phys. Rev. Lett. **57**, 1284 (1986).

[10] M. Franaszek, Phys. Rev. **A46**, 6340 (1992); M. Franaszek and A. Phys. Lett. **A178**, 85 (1993); **A182**, 99 (1993).

[11] K. G. Szabó and T. Tél, Phys. Lett. **A196**, 173 (1994); K. G. Szal Lai, T. Tél and C. Grebogi, Phys. Rev. Lett. **77**, 3102 (1996)

[12] C. Grebogi et al, Phys. Rev. Lett. **50**, 935 (1983), E. Ott et al, Ph Lett. **71**, 4134 (1993).

[13] C. Grebogi et al, Lect. Notes in Math. **1342**, 220 (1988).

[14] E. Ott and T. Tél, Chaos **3**, 417 (1993), and the entire special issue o no.4 (1993).

[15] C. Jung and E. Ziemniak, J. Phys A **25** (1992), 3929; C. Jung, T. Té Ziemniak, Chaos **3** (1993), 555; E. Ziemniak, C. Jung and T. Tél, Pl **76** (1994), 123.

[16] Á. Péntek, T. Tél, and Z. Toroczkai, J. Phys. A **28** (1995), 2191; Fra 33 (1995).

[17] Á. Péntek, Z. Toroczkai, T. Tél, C. Grebogi and J. Yorke, Phys. Rev. E

[18] M. Iansiti et al, Phys. Rev. Lett. **55**, 746 (1985); H. Herzel et al., Z. forsch. **42a**, 136 (1987); A. R. Bulsara et al., Phys. Rev. **A42**, 4614 M. Frey and E. Simiu, in: *Spatio-Temporal Patterns*, ed.: P. E. Cladis Palffy-Muhoray (Addison-Wesley, 1995); E. Simiu and M. Franaszek, Engineering Technical Conferences **84**, 897(1995).

[19] R. W. Leven, B. Pompe, C. Wilke and B. P. Koch, Physica (Amsterc **16**, 371 (1985).

[20] P. J. Widmann, M. Gorman and K. A. Robbins, Physica (Amsterdam) **D 36**, 157 (1989).

[21] T. L. Carroll, L. M. Pecora and F. J. Rachford, Phys. Rev. Lett. **59**, 2891 (1987).

[22] Z. J. Kowalik, M. Franaszek and P. Pieranski, Phys. Rev. **A 37**, 4016 (1988).

[23] W. L. Ditto et al., Phys. Rev. Lett. **63**, 923 (1989).

[24] R. Stoop and J. Parisi, Phys. Rev. **A 43**, 1802 (1991).

[25] Y. Wang, J. Singer, and H. H. Bau, J. Fluid. Mech. **237**, 479 (1992).

[26] J. Wang, P. G. Sorensen, and F. Hynne, J. Chem. Phys. **98**, 725 (1994).

[27] I. M. Jánosi, L. Flepp, and T. Tél, Phys. Rev. Lett. **73**, 529 (1994).

[28] R. W. Leven and M. Selent, Chaos Sol. Frac. **4**, 2217 (1994)

[29] J. C. Sommerer, H-C Ku, and H. E. Gilreath, Phys. Rev. Lett. **77** 5055 (1996).

[30] G. Stépán, Vehicle System Dynamics **20**, 341 (1991), in: *Future Direction of Nonlinear Dynamics in Physical and Biological Systems* (Plenum, New York, 1992): L. Palkovics, G. Stépán, and P. Michelberger, Machine Vibration **2**, 47 (1993)

[31] H. E. Nusse and J. Yorke, Physica **36D**, 137 (1989).

[32] Jacobs, E. Ott, and C. Grebogi, ...

[33] E. Ott, C. Grebogi, and J. Yorke, Phys. Rev. Lett **64**, 1196 (1990)

[34] K. Pyragas, Phys. Lett. **170A**, 421 (1992).

[35] Z. Toroczkai, Phys. Lett. **190A**, 71 (1994); B. Sass and Z. Toroczkai, J. Phys. **A29**, 3545 (1996)

[36] T. Tél, J. Phys. **A24**, L1359 (1991).

[37] I. Z. Kiss, V. Gáspár, L. Nyikos, and P. Parmanananda, J. Phys. Chem. xxxx (1997)

[38] T. Tél, Int. J. Chaos Bifurcations **3**, 757 (1993)

[39] G. Pianigiani and J. A. Yorke, Trnas AMS. **252**, 351 (1979).

[40] Z. Kovács, K. G. Szabó, and T. Tél, in: *Nonlinearity and Chaos in Engineering Dynamics*, ed.: J. M. T. Thompson and S. R. Bishop (Wiley and Sons, Chichester, 1994) p. 155

[41] M. Ding, E. Ott, and C. Gebogi, Phys. Rev. **E50**, 4228 (1994)

[42] Y.-C. Lai, T. Tél, and C. Grebogi, Phys. Rev. **E48** 709 (1993).

[43] Y.-C. Lai, C. Grebogi and T. Tél, in: *Towards the Harnessing of C* M. Yamaguti (Elsevier, Amsterdam, 1994) p. 153.

[44] F. J. Romeiras, C. Grebogi, E. Ott, and W. Dayawansa, Physi 165(1992); D. Auerbach, C. Grebogi, E. Ott and J. A. Yorke, Ph Lett. **69**, 3479(1992).

[45] Y.-C. Lai, C. Grebogi, J. A Yorke, and I. Kan, Nonlinearity **6**, 1 (19

[46] Y.-C. Lai and C. Grebogi, Phys. Rev. E **49**, 1094 (1994).

[47] Y. C. Lai and C. Grebogi, Phys. Rev. E **47**, 2357(1993).

[48] N. J. Mehta and R. M. Henderson, Phys. Rev. A **44**, 4861(1991)

[49] H. Wang, E. H. Abed, and A. M. A. Hamdan, *Proc 1992 American Conference* (Chicago), pp. 2084-2088 (1992); H. Wang and E. H. Abe *NOLCOS'92: Nonlinear Control System Design Symposium*, Ed. M Bordeaux, France, pp. 57-62 (1992).

[50] K. McCann and P. Yodzis, Ame. Naturalist **144**, 873 (1994).

[51] M. Dhamala and Y.-C. Lai, "Controlling transient chaos in determinis with applications to electrical power systems and ecology," preprint (

[52] S. Hayes, C. Grebogi, and E. Ott, Phys. Rev. Lett. **70**, 3031 (1993); S C. Grebogi, E. Ott, and A. Mark, Phys. Rev. Lett. **73**, 1781 (1994); I S. Hayes, and C. Grebogi, Phys. Rev. Lett. **78**, 1247 (1997); E. B Dolnik, Phys. Rev. E **55**, 6404 (1997); E. Bollt, Y.-C. Lai, and C. C Phys. Rev. Lett. **79**, 3787 (1997); E. Bollt, Y.-C. Lai, Phys. Rev. E **5** (1998).

[53] S. Taherion and Y.-C. Lai, "Communicating with transient chaos," I (1998).

[54] J. Kadtke, Á. Péntek, and G. Pedrizzetti, Phys. Lett **204A**, 108 (19 Péntek, J. Kadtke, and G. Pedrizzetti, Phys. Rev. **E58**, 1883 (19 Péntek, PhD Thesis, University of California, San Diego, 1998

[55] D. Reznik and E. Schöll, Z. Phys. **B91**, 309 (1993).

[56] T. R. Kopp, PhD Thesis, University of Frankfurt am Main, 1998 (in G

[57] Y.-C. Lai, M. Ding, and C. Grebogi, Phys. Rev. E **47**, 86 (1993).